JMEPEG (2023) 32:9011–9018
https://doi.org/10.1007/s11665-022-07792-3

1059-9495/$19.00

TECHNICAL ARTICLE

Wear and Corrosion of UNS S32750 Steel Subjected to Nitriding and Cathodic Cage Deposition

Lauriene G.L. Silva, M. Naeem, Thércio H.C. Costa, Maxwell S. Libório, Rafael M. Bandeira, Natália S. Ferreira, Luciana S. Rossino, César A.A. Júnior, José C.A. Queiroz, João F.M. Neto, and Rômulo R.M. Sousa

Submitted: 16 May 2022 / Revised: 20 October 2022 / Accepted: 11 November 2022 / Published online: 4 January 2023

Super duplex stainless steel (SDSS) has excellent corrosion resistance and good mechanical properties. However, the tribological characteristics of these steels reduce their applicability. Plasma nitriding (PN) and cathodic cage deposition (CCPD) have been used to cause surface changes to improve wear resistance without significant loss of corrosion resistance. In this study, PN and CCPD treatments were performed at 350 and 450 °C to evaluate the influence of temperature on wear and corrosion resistance. Microhardness, XRD, SEM, wear, and corrosion tests were performed to evaluate the results. It was observed that the treatments adopted in the study improved the hardness and wear resistance of all samples. The results showed that nitriding performed well in terms of corrosion resistance at low temperatures (350 °C), while at higher temperatures (450 °C), the duplex treatment proved to be more suitable.

Keywords CCPD, corrosion resistance, plasma nitriding, stainless steel, wear resistance

1. Introduction

Super duplex stainless steels (SDSS) exhibit a microstructure composed of austenite and ferrite phases with a ratio of approximately 1:1 (Ref 1). With a high content of Chromium (24-27%) and also the presence of nickel, manganese, and nitrogen (Ref 2), mainly concentrated in the austenite phase, these steels are widely used in aggressive environments, especially in the oil and gas industry (Ref 3-5), and currently, in industrial of paper and cellulose (Ref 6), where there is a need for mechanical components with good strength, toughness and corrosion resistance since these steels present greater resistance to chemical attacks due to the formation of chromium oxide on the steel surface in the presence of oxygen (Ref 7).

The economic value of SDSS steels varies less due to nickel's lower composition content than austenitic stainless steels and nickel-based alloys (Ref 8, 9). Although stainless steels have good mechanical strength (Ref 10-12), they do not meet all project specifications in many industrial applications and are still limited (Ref 13).

In this context, surface treatments of stainless steel are necessary to improve hardness, tribological behavior, and fatigue resistance, avoiding the degradation of corrosion resistance (Ref 14, 15). Among these treatments, plasma nitriding (PN) offers the possibility of modifying the surface properties by controlling the processing parameters without altering the core bulk structure (Ref 16, 17). However, due to the high chromium content in SDSS steels, nitride layers tend to form due to the intense binding energy between chromium and nitrogen. Thus, chromium nitride precipitation occurs, decreasing corrosion resistance and/or mechanical properties (Ref 18, 19).

Low-temperature nitriding inhibits the formation of Cr nitride due to substitutional Cr diffusion, while the interstitial atoms can diffuse under so-called para-equilibrium conditions, and supersaturated solid solutions of the diffuse interstitial atoms in austenite can be obtained, which allow an increase in surface hardness without harming corrosion (Ref 20, 21).On the other hand, processes that reduce the austenite content to approximately 25% are unacceptable for most industrial applications due to the substantial reduction in corrosion resistance (Ref 1).

In addition to nitriding, another technique is cathodic cage plasma deposition (CCPD), which provides better wear and corrosion performance. In this technique, the material from the cage is pulled out due to the formation of the hollow cathode effect in its holes, combined with the elements of the atmosphere, and then deposited on the surface of the substrate. Therefore, if a titanium cage is used, the substrate is coated with a film composed of Ti-containing phases, and consequently, better surface properties can be acquired (Ref 22, 23).

OskanGokcekaya et al. (2022) performed plasma nitriding in an atmosphere with 80%N2-20%H2 at 450, 500, and 550 °C for 2, 4, and 9 h of treatment. Due to temperature and treatment time, the results showed variation in the relative amount of

Lauriene G.L. Silva and **Rômulo R.M. Sousa**, Federal University of Piauí, Postgraduate Program in Materials Science and Engineering, Teresina, PI, Brazil; **M. Naeem**, Department of Physics, Women University of Azad Jammu and Kashmir, Bagh, Pakistan; **Thércio H.C. Costa** and **José C.A. Queiroz**, Department of Mecanics, Federal University of Rio Grande Do Norte, Natal, RN, Brazil; **Maxwell S. Libório**, School of Science and Technology, Federal University of Rio Grande Do Norte, Natal, RN, Brazil; **Rafael M. Bandeira** and **Natália S. Ferreira**, Chemistry Department, Federal University of Piauí, Teresina, PI, Brazil; **Luciana S. Rossino** and **César A.A. Júnior**, Federal University São Carlos – UFSCar, Sorocaba, SP, Brazil; **João F.M. Neto**, Federal University of Rio Grande Do Norte, Postgraduate Program in Materials Science and Engineering, Natal, RN, Brazil. Contact e-mail: cesar.augusto.049@ufrn.edu.br.

austenite, expanded austenite, ferrite, and nitride precipitates (Ref 24).In high-temperature treatments, nitrogen diffusion to ferritic stainless steel (ccc) leads to the formation of iron nitrides (ε—Fe_2-3 N, γ'- Fe_4N) and nitrides such as CrN, which improve hardness but impair corrosion resistance. On the other hand, in treatments with temperatures below 450 °C, the entry of nitrogen into the stainless steel structure causes the formation of the expanded austenite phase (γN), responsible for maintaining corrosion resistance and increasing hardness (Ref 25, 26). The review work by L. H. P. Abreu et al. (2020) presented several results that used the CCPD technique to produce homogeneous and wear-resistant titanium nitride (TiN) films. Despite producing thinner layers than conventional nitriding, the TiN films produced by CCPD have high hardness, and their homogeneity acts as a barrier, reducing oxygen access in the innermost regions and susceptible to corrosion degradation (Ref 22, 27, 28). The combination of conventional plasma nitriding and CCPD, duplex treatment, can be adopted to add the benefits caused by each of the treatments to make the steel surface more resistant to wear without losing its corrosion resistance.

This study aims to contribute to understanding the duplex treatment (PN + CCPD) with emphasis on the influence of temperature on the tribological behavior and corrosion resistance of UNS S32750 steel. The presented methodology suggests an evaluation of the mechanical properties and the structural modification as a function of the treatment temperature change (350 to 450 °C) in order to improve the wear resistance without loss of corrosion resistance.

2. Material and Experimental

This work used super duplex stainless steel, UNS S32750, with a nominal composition shown in Table 1.

Cylindrical samples of super duplex steel were prepared according to metallographic techniques to produce a reduction of irregularities in the pieces, as described by Leonardo C. Silva (Ref 29). After the preparation of the samples, one was separated to be the standard sample (Base), another was submitted only to CCPD, and the remaining were submitted to the treatment of ionic nitriding. Before the treatments, the samples were cleaned in the plasma chamber by sputtering with an argon atmosphere for 30 min to remove surface impurities. Then, the samples were nitrided for 4 h in an atmosphere resulting from a flow of $17H_2/51N_2$ and a working pressure of 2 mBar. However, the temperature was the modifying factor of the nitrided layers, as indicated in Table 2. Then the N350 and N450 samples, respectively nitrided at 350 and 450 °C, were treated using the plasma deposition technique with a titanium cathodic cage (Table 2). In the deposition, the parameters were set as follows: $40H_2/20N_2$, 2 h, and 1.5 mBar.

The system used for the treatments consists of a plasma reactor with peripheral equipment (a set of electronic sensors, a gas supply system, a vacuum pump, and a voltage source) duly described in previous works (Ref 23, 30, 31). The samples used in the study were subjected to a chemical attack with Behara reagent (20 ml of hydrochloric acid, 80 ml of distilled water, and 1 g of potassium metabisulfite) to reveal microstructure in optical microscopy analysis to measure the thickness of the formed layers. Four measurements were made along the films to obtain the average value. These analyzes were performed in an Olympus optical microscope, model BX60M. Microhardness was performed according to ASTM E92 and ASTM E384 standards using an INSIZE microhardness tester, model ISH-TDV 1000 (Ref 32). Five measurements were made from the center to the edge, with a load of 0.98 N, the mean value, and their respective standard deviations to evaluate treatment effects along the surface. X-ray diffraction was performed with a Shimadzu diffractometer (model DRX-7000) with CuKα radiation, voltage 40 kV, current 40 mA, angular range (2θ) 30-100°.

The ball-on-disk wear test was performed with 52,100 steel balls (C = 0.98-1.1%, Fe = 97.05%, Cr = 1.4%, Si = 0.25%, P ≤ 0.025%, Mn = 0.35%, S ≤ 0.25%) and 25.4 mm in diameter to obtain the wear volume and friction coefficient of the treated samples (Ref 33). The parameters used to perform the test were 8 N of normal load, and 40 Hz (160 RPM) of rotation, without any abrasive or lubricant. The wear tests were performed by varying the test time in 2, 5, 10, 15, 20, 25, and 30 min, keeping the tested region fixed to observe the wear resistance of the samples to the analyzed time(Ref 34-37). The method adopted in this analysis is described in detail in previous works (Ref 36, 38, 39). The corrosion test was performed in a three-electrode electrolytic cell (3.5% NaCl solution) for 2 h. Then, potentiodynamic polarization measurements of the samples were performed, starting the scan at 250 mV below the OCP, with a rate of 1 mV/s, until reaching a current of 1 mA/cm2. Each measurement was performed in triplicate to verify test repeatability. In this assay, measurements

Table 1 Nominal chemical composition of UNS S32750 super duplex steel (% mass) (Ref. 30)

Material	Cr	Mo	Ni	C	N	Mn	Si	P	S	Fe
UNS S32750	24.6	3.49	6.7	0.09	0.29	0.76	0.27	0.02	0.001	Bal

Table 2 Treatment parameters for ion nitriding on UNS S32750 super duplex steel

Samples	Base	N1	N2	N350	N3	N4	N450	
Temperature, °C	…		350			450		
Samples			**ND350**			**ND450**		**D450**
Temperature, °C			350			450		450

Table 3 Microhardness of steel samples UNS S32750 after plasma deposition treatment

Samples	Microhardness, HV			Standard deviation, S
	Minimum	Average	Maximum	
BASE	348,98	380,01	418,25	25,85
N1	504,90	550,04	578,15	28,11
N2	574,74	645,11	743,97	84,60
ND.350	675,74	736,94	825,03	63,13
N3	1321,63	1569,37	1819,65	190,18
N4	1305,99	1354,64	1421,66	44,64
ND450	1107,23	1359,38	1509,12	153,08

of open circuit potential (OCP) and potentiodynamic polarization curves were obtained before and after treatments.

3. Results and Discussion

The analysis of the microhardness results is presented in Table 3, considering the minimum, average, maximum microhardness, and the standard deviation (S) of the samples.

According to the hardness values obtained, the treatments favored the increase in the surface hardness of the SDSS, since all the treated samples had a higher microhardness value than the untreated SDSS. The temperature increase from 350 to 450 °C in the nitriding process caused a significant increase in surface hardness. This effect is justified by the increase in diffusion and consequent mobility of nitrogen to the innermost regions of the sample, forming the expanded austenite phase (γ_N) (Ref 37). In addition, nitrogen diffusion also causes the formation of iron nitrides (ε—Fe_{2-3} N, γ'- Fe_4N) (Ref 31, 40). The sample submitted to post-treatment of CCPD with titanium cage at 350 °C (sample ND350) showed a small increase in hardness compared to samples only nitrided due to the small thickness of the TiN film, showing that the hardness of the nitride film of titanium is superior to the hardness of the nitrided layer formed at this temperature. On the other hand, the surface hardness obtained in the sample ND450 did not increase in the samples, only nitrided. This fact can be explained because the hardness of the nitrided layer at 450 °C presented a value similar to the hardness value of titanium nitride films, as reported by Libório et al. (2020) (Ref 41).

The x-ray diffraction analysis of the nitrided samples at 350 and 450 °C showed expanded ferrite and austenite crystalline phases characterized by the shift of the α and γ phase peaks to a low angle 2θ, in addition to iron nitride precipitated phases (type ε and γ') as shown in Fig. 1 (Ref 42). The diffractograms confirmed that the increased processing temperature contributed to the greater diffusion of interstitial nitrogen in the nitrided layer. However, the temperatures reached did not favor the formation of chromium precipitates, which would cause a significant reduction in the corrosion resistance of the SDSS. Figure 1 also highlights the increase in displacement of the main ferrite and austenite peaks, respectively, at 43.43 and 44.53°, as a function of temperature. This result points to the saturation of nitrogen in the iron matrix and a subsequent tendency toward a more intense formation of Fe_xN and Cr_xN (Ref 43).

The cut made in the cross section made it possible to analyze the treated samples' microstructure and visualize the modified surface layers. Figure 2 shows the microstructure of sample N350 composed of ferrite and austenite lamellae oriented horizontally due to the lamination process. However, a thin and homogeneous nitrided layer resulting from low nitrogen diffusion is observed. The CCPD deposition treatment performed on the nitrided sample at 350 °C contributed to the increase in the layer from 2.27 to 4.65 μm (Fig. 2c). Despite the small increase in surface hardness that justifies the presence of deposited thin film, it cannot be seen in the images obtained in this analysis. Figure 2(b) shows the cross section of sample N450 (only nitrided). A significant increase in the nitrided layer is observed due to the increase in the nitriding temperature (approximately 25.5 μm) (Ref 44).This sample presents lamellae in the vertical direction, causing the composition of the nitride layer formed by expanded ferrite and expanded austenite to be oriented in this direction(Ref 45). Among the analyzed samples, N450 showed compromised homogeneity due to the noticeable fracture of the layer in the superficial region. The ND450 sample, unlike the N450 sample, was exposed to deposition nitriding treatments with the lamellae oriented horizontally. However, the layer thickness of this sample reached a value similar to the sample, only nitrided at the same temperature (N450) but with greater homogeneity.

Figure 3 shows the surface optical microscopy and electron microscopy of the cross section of the sample N450, highlighting the contrast and the distribution of the ferrite (dark) and austenite (light) phases of the UNS S32750 steel. Using ImageJ software to calculate the percentage of phases observed on the surface of the sample, with the measurement of 10 different areas, the result of 50.81% of austenite phase was obtained, representing the proportion approximately indicated in the literature for the stainless steel studied (Ref 46, 47).

Figure 4 shows that the tribological analysis during the test time increases the amount of wear because the longer the sample is subjected to the test, the greater the wear it will suffer. The treatments improved the wear resistance of the base material, demonstrating that the plasma treatments of both conventional nitriding (N) and duplex treatments (ND) had similar behaviors. Efficient in increasing the wear resistance of the material.

Figure 4(b) shows that sample N450 obtained better wear resistance (0.010 mm^3) between treatments, showing lower wear volume values as a test time function. On the other hand, the deposition of the TiN deposited film only showed a higher volume of wear (0.043 mm^3). Therefore, lower wear resistance, different from the samples only nitrided and submitted to the duplex treatment. It is also observed that samples N350 and N450 presented tribological behavior with an insignificant difference.

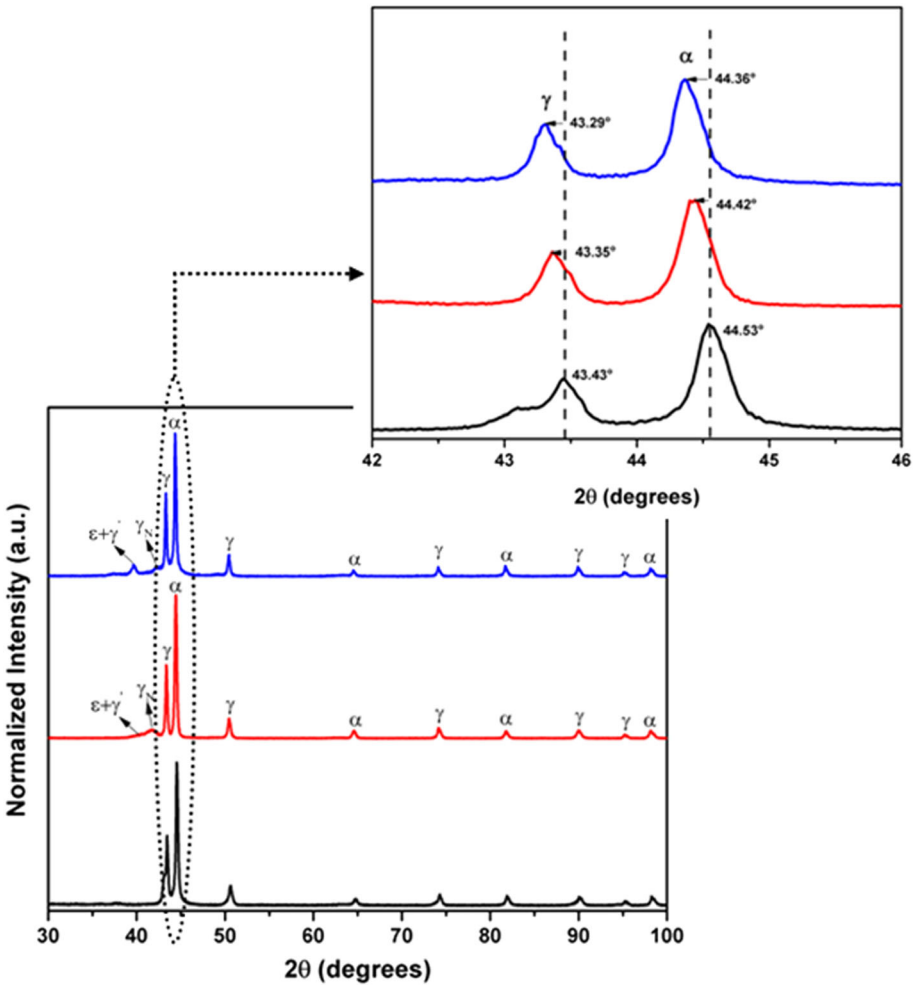

Fig. 1 Diffractogram of nitrided UNS S32750 steel samples

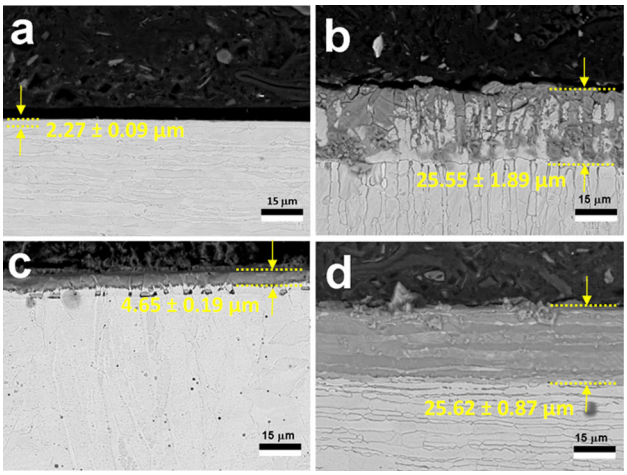

Fig. 2 Cross-sectional images of samples subjected to nitriding and duplex treatment: (a) N350, (b) N450, (c) ND350, and (d) ND450

The wear marks of the base material, nitrided samples, and duplex-treated samples are shown in Fig. 5. It shows that the base material is severely worn and damaged, and a wide wear track is formed. In addition, the entire wear track appears to be scratched. In contrast, the wear tracks of the treated samples (c, d, and f) are relatively narrow, and the surface is less damaged and appears homogeneous. The improvement in wear behavior can be credited to an increase in hardness, as shown in Table 3, due to the formation of hard nitrides on the surface. but this moderate wear with harder surfaces favors abrasive wear. The further improvement in hardness behaviors can be attributed to the deep diffusion of nitrogen, which creates a hardness gradient with the core. This hardness gradient increases the adhesion of the coating to the substrate.

Among the results obtained with the duplex treatment (nitriding + deposition), the best result was obtained with the condition at 450° C, presenting a lower volume of wear as a function of the test time used, which is in accordance with the values of surface hardness reported in Table 3. This result points to the formation of a light ceramic layer of TiN formed on the surface due to plasma deposition with a cathodic cage.

Figure 6 shows the coefficient of friction obtained through the test carried out with a fixed time of 15 min. The samples treated at 350 °C (N350 and ND350) and the D450 showed a higher friction coefficient than the base sample over 15 min of tribological testing. This fact can be explained by the formation of the layers in these samples having hardness values lower than the hardness of the 52,100 steel ball (∼ 700 HV) used in the ball-on-disk tribological test (Ref 48). This factor may have contributed to removing hard particles from the nitrided layer and mainly from the TiN film present in samples D450 and

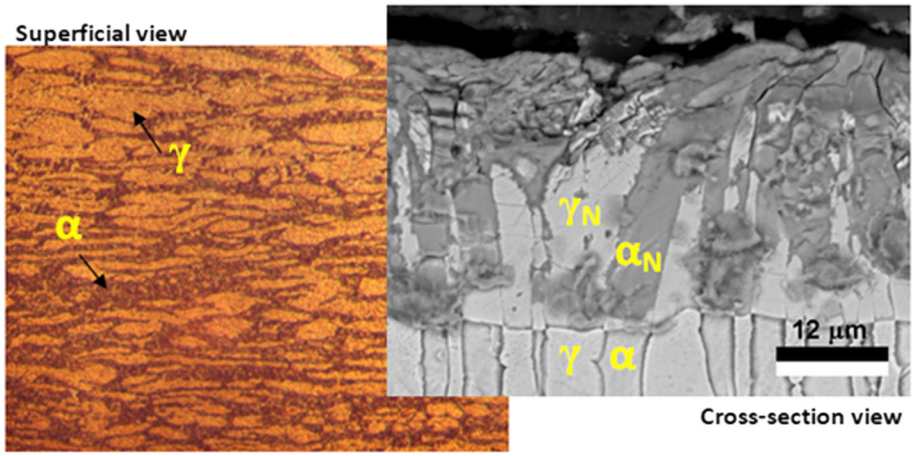

Fig. 3 surface view with emphasis on the ferrite and austenite phases and cross-sectional view of the layer formation guided by the phases of the base material

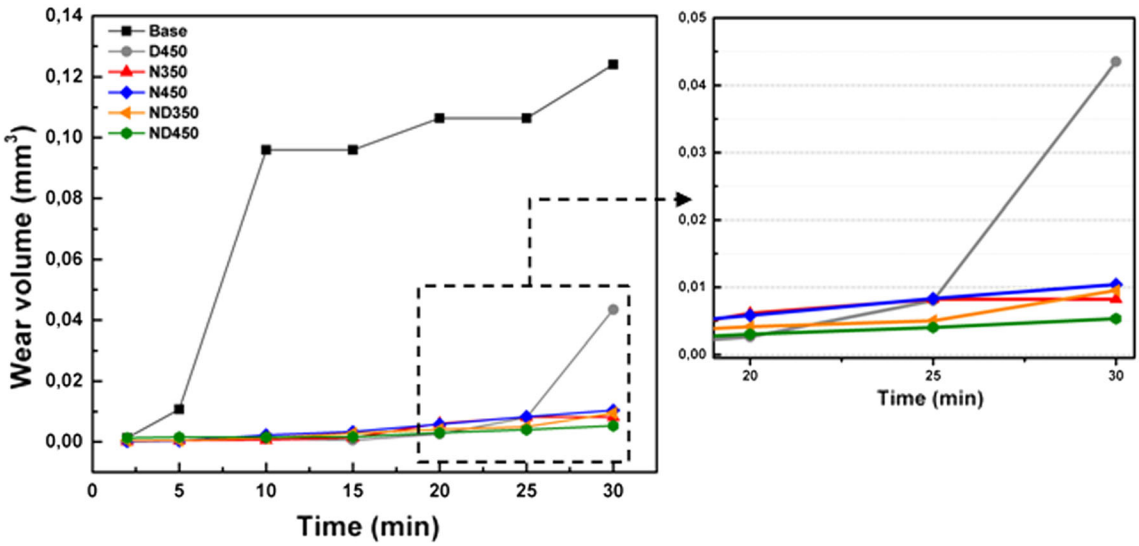

Fig. 4 Wear volume vs. function of time: (a) test from 0 to 30 min; (b) enlargement of the graph in the region of the end of the assay

ND350. However, despite removing debris-forming particles, this did not result in a high loss of surface material. Furthermore, after 400 s of testing, the sample N350 showed a reduction in the coefficient of friction. This fact is consistent with the hypothesis of progressive removal of the thin nitride layer and convergence of the tribological behavior of this sample with the base sample at the end of the test (Ref 29, 49). Samples N450 and ND450, on the other hand, had a lower friction coefficient than the previous samples. This reduction is associated with its layers' high hardness and thickness, as already reported in the hardness and SEM analyses. The hardness of the samples treated at 450 °C showed high wear resistance, and its behavior remained stable over time due to the high thickness of the layers.

Open circuit potential (OCP) measurements were made to investigate the stability of the electrodes with and without treatment. Stable films, in general, present more positive OCP values, with potential shifted in the anodic direction. Figure 7 shows the OCP curves of the different samples submitted to the 3.5% NaCl solution. It was verified that the sample subjected to nitriding at 350 °C had the highest OCP value (0.09 V) among the other samples, indicating that at a temperature of 350 °C, the nitriding process is efficient for the formation of stable films. On the other hand, the sample nitrided at 450 °C exhibited a significant decrease in the potential to -0.37 V. The rapid decrease in the OCP value at this temperature is a consequence of the unstable nature of the formed film is more susceptible to corrosion. For comparison purposes, the OCP curve of the titanium nitride-coated substrate at 450 °C (D450) is shown. Interestingly, the titanium nitride film alone is no longer efficient in the surface passivation process, presenting an OCP of -0.28 V. However, the results of the duplex treatment indicate that there was a synergistic effect that led to the formation of a more stable film for the treatment carried out at 450 °C. In contrast, the ND350 sample reveals that the duplex treatment process is not effective for forming a surface that is less susceptible to corrosion.

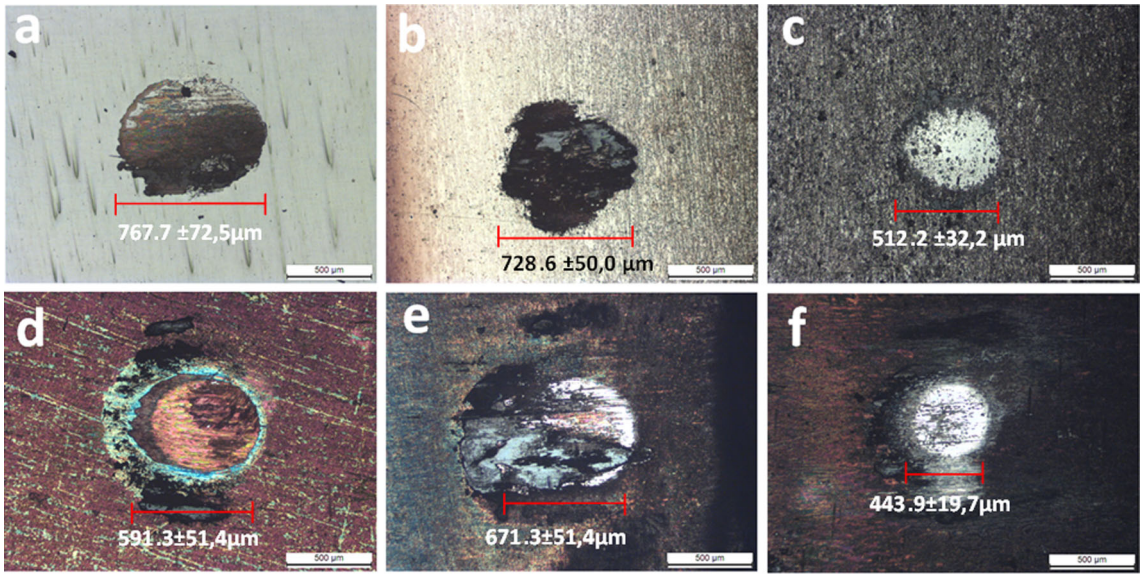

Fig. 5 Optical micrographs of wear tracks of (a) Base; (b) N350; (c) ND350; (d) D450; (e) N450; (f) ND450

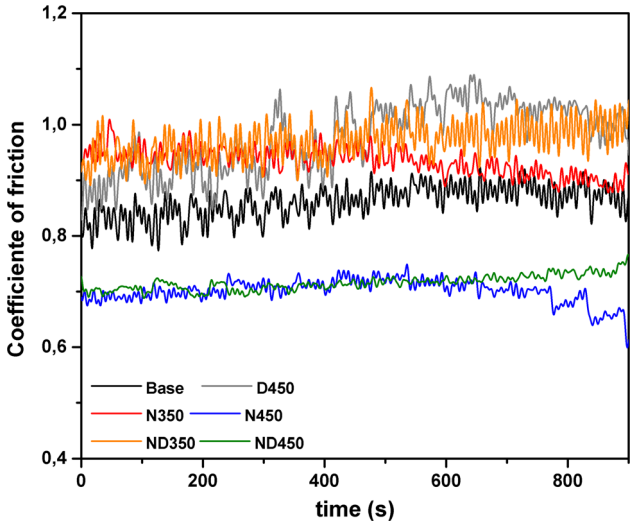

Fig. 6 Coefficient of friction of samples over 15 min of the tribological test

Figure 7(b) shows the relationship between E_{corr} (corrosion potential) and J_{corr} (current density) for each sample studied. As reported in Fig. 7(a), the sample only nitrided at 350 °C has better corrosion resistance because it has a more positive corrosion potential than all other samples. The speed of corrosion reactions in samples N350 and D450 and the Base sample is close (on the scale of 9×10^{-9} (Log A.cm^{-2})). On the other hand, samples N450, ND350, and ND450 showed higher corrosion rates with current density on the scale of 10^{-8} for ND350 and ND450 and on the scale of 10^{-7} for sample N450.The values obtained in the corrosion test for the corrosion potential and current density are described in Table 4.

4. Conclusions

The technique adopted in this work, composed of nitriding and deposition by a cathodic cage of TiN, resulted in a superficial modification of the mechanical and electrochemical

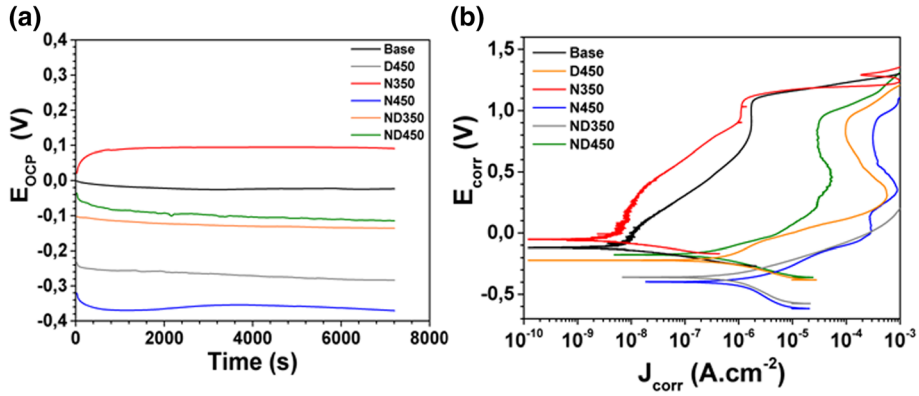

Fig. 7 (a) Open circuit potential (OCP) measurements, and (b) Potentiodynamic polarization curves measurements of the samples surface with and without treatment

Table 4 Corrosion potential and current density values of the samples

Sample	Base	D450	N350	N450	ND350	ND450
E_{corr}, mV	−125	−355	−59	−397	−219	−178
j_{corr}, A/cm^2	4.1×10^{-9}	6.7×10^{-7}	4.3×10^{-9}	8.8×10^{-7}	3.6×10^{-7}	2.5×10^{-7}

properties of the UNS S32750 steel. Because of the results obtained, it can be concluded that:

- Plasma nitriding treatment and duplex treatment at 350 and 450 °C promote an increase in the surface hardness of UNS S32750 steel due to the formation of phases resulting from the insertion of nitrogen in the crystal lattice of stainless steel without the formation of precipitates such as CrN that are detrimental to corrosion resistance;
- The thickness of the layers produced by the treatments and their compositions influenced the tribological behavior of the samples, improving the wear resistance as reported in the ball-disk test;
- The coefficient of friction is a parameter strongly influenced by the hardness of the tribological pair (Steel 52,100 and sample), thickness, and composition of the layers produced;
- Despite the better tribological performance, the samples showed variations in corrosion resistance. For example, sample N350 showed the best performance in the corrosion test, while sample N450 showed the worst performance, showing that the temperature variation from 350 to 450 °C causes significant changes in corrosion resistance. However, the ND450 sample showed a corrosion potential close to the base sample.

Finally, it is concluded that the methodology adopted in this work is efficient for improving the mechanical strength and tribological performance of UNS S32750 steel. However, nitriding presents a good performance regarding corrosion resistance at low temperatures (350 °C), while at higher temperatures (450 °C), the duplex treatment showed promise.

Funding

This study was financed in part by the Coordenação de Aperfeiçoamento de Pessoal de Nível Superior—Brasil (CAPES)—Finance Code 001.

Conflict of interest

No potential conflict of interest was reported by the author(s).

References

1. F.M.R. Borges, W.F.A. Borges, R.L.P. Santos, V.S. Leal, J.R. dos Santos Júnior, A.O. Lobo, and R.R.M. de Sousa, Corrosion Resistance and Microstructural Evaluation of a Plasma Nitrided Weld Joint of UNS S32750 Super Duplex Stainless Steel, *Mat. Res.*, 2021, **6**, p 45614. https://doi.org/10.1590/1980-5373-MR-2021-0087
2. G.S. da Fonseca, P.M. de Oliveira, M.G. Diniz, D.V. Bubnoff, and J.A. de Castro, Sigma Phase in Superduplex Stainless Steel: Formation, Kinetics and Microstructural Path, *Mat. Res.*, 2017, **20**, p 249–255.
3. D. Martínez, R. Gonzalez, K. Montemayor, A. Juarez-Hernandez, G. Fajardo, and M.A.L. Hernandez-Rodriguez, Amine Type Inhibitor Effect on Corrosion-Erosion Wear in Oil Gas Pipes, *Wear*, 2009, **267**(1), p 255–258.
4. R. Barker, X. Hu, A. Neville, and S. Cushnaghan, Empirical Prediction of Carbon-Steel Degradation Rates on an Offshore Oil and Gas Facility: Predicting CO_2 Erosion-Corrosion Pipeline Failures Before They Occur, *SPE J.*, 2013, **19**(03), p 425–436.
5. A.B. Tahchieva, N. Llorca-Isern, and J.-M. Cabrera, Duplex and Superduplex Stainless Steels: Microstructure and Property Evolution by Surface Modification Processes, *Metals*, 2019, **9**(3), p 347.
6. Y.S. Sato, T.W. Nelson, C.J. Sterling, R.J. Steel, and C.-O. Pettersson, Microstructure and Mechanical Properties of Friction Stir Welded SAF 2507 Super Duplex Stainless Steel, *Mater. Sci. Eng., A*, 2005, **397**(1), p 376–384.
7. F. Borgioli, The "Expanded" Phases in the Low-Temperature Treated Stainless Steels: A Review, *Metals*, 2022, **12**(2), p 331.
8. Z. Schulz, P. Whitcraft, and D. Wachowiak Availability and Economics of Using Duplex Stainless Steels. (Texas, USA), OnePetro, 2014, https://onepetro.org/NACECORR/proceedings/CORR14/All-CORR14/NACE-2014-4345/123141
9. M. Snis and J. Olsson, Reduce Costs for Storage and Distribution of Desalted Water — Use Duplex Stainless Steel, *Desalination*, 2008, **223**(1), p 476–486.
10. R. Abdolvand, M. Atapour, and M. Shamanian, Effects of Cooling Regimes on the Microstructural and Mechanical Properties of the Transient Liquid Phase Joints of UNS S32750 Super Duplex Stainless Steel/BNi-2/AISI 304 Stainless Steel, *J Mater Sci*, 2022, **57**(6), p 4383–4398.
11. S. Saravanan, K. Raghukandan and N. Sivagurumanikandan, Pulsed Nd: YAG Laser Welding and Subsequent Post-Weld Heat Treatment on Super Duplex Stainless Steel, *J. Manuf. Process.*, 2017, **25**, p 284–289.
12. M.F. McGuire, *"Stainless Steels for Design Engineers", (USA)*, ASM International, New York, 2008
13. C.B. von der Ohe, R. Johnsen, and N. Espallargas, Multi-Degradation Behavior of Austenitic and Super Duplex Stainless Steel – The Effect of 4-Point Static and Cyclic Bending Applied to a Simulated Seawater Tribocorrosion System, *Wear*, 2012, **288**, p 39–53.
14. M.Z. Babur, Z. Iqbal, M. Shafiq, M.Y. Naz, and M.M. Makhlouf, Hybrid TiN-CCPN Coating of AISI-201 Stainless Steel by Physical Vapor Deposition Combined with Cathodic Cage Plasma Nitriding for Improved Tribological Properties, *J. Build. Eng.*, 2022, **45**, p 103512.
15. A.M.S. Dias, E.C. Silva, and M.S. Libório, Experimental-Numerical Technique to Evaluate the Thickness of TiN Thin Film, *Mat. Res.*, 2019, **22**, p 4561. https://doi.org/10.1590/1980-5373-MR-2018-0283
16. M. Tsujikawa, D. Yoshida, N. Yamauchi, N. Ueda, T. Sone, and S. Tanaka, Surface Material Design of 316 Stainless Steel by Combination of Low Temperature Carburizing and Nitriding, *Surf. Coat. Technol.*, 2005, **200**(1), p 507–511.
17. J. Wang, Y. Lin, D. Zeng, J. Yan, and H. Fan, Effects of the Process Parameters on the Microstructure and Properties of Nitrided 17–4PH Stainless Steel, *Metall. Mater. Trans. B*, 2013, **44**(2), p 414–422.
18. E. de Araújo, R.M. Bandeira, M.D. Manfrinato, J.A. Moreto, R. Borges, S.S. Vales, P.A. Suzuki, and L.S. Rossino, Effect of Ionic Plasma Nitriding Process on the Corrosion and Micro-Abrasive Wear Behavior of AISI 316L Austenitic and AISI 470 Super-Ferritic Stainless Steels, *J. Mater. Res. Technol.*, 2019, **8**(2), p 2180–2191.
19. H.-J. Spies, C. Eckstein, and H. Zimdars, Structure and Corrosion Behaviour of Stainless Steels after Plasma and Gas Nitriding, *Surf. Eng.*, 2002, **18**(6), p 459–460.
20. G.M. Michal, F. Ernst, H. Kahn, Y. Cao, F. Oba, N. Agarwal, and A.H. Heuer, Carbon Supersaturation Due to Paraequilibrium Carburization: Stainless Steels with Greatly Improved Mechanical Properties, *Acta Mater.*, 2006, **54**(6), p 1597–1606.
21. F.N. Jespersen, J.H. Hattel, and M.A.J. Somers, Modelling the Evolution of Composition-and Stress-Depth Profiles in Austenitic Stainless Steels during Low-Temperature Nitriding, *Modelling Simul, Mater. Sci. Eng.*, 2016, **24**(2), p 025003.

22. M.G.C. Barbosa, B.C. Viana, F.E.P. Santos, F. Fernandes, M.C. Feitor, T.H.C. Costa, M. Naeem, and R.R.M. Sousa, Surface Modification of Tool Steel by Cathodic Cage TiN Deposition, *Surf. Eng.*, 2021, **37**(3), p 334–342.
23. E.S. Costa, R.R.M. de Sousa, R.M. Monção, M.S. Libório, and T.H.C. Costa, Plasma Nitriding and Deposition in AISI M_2 and D_2 Steel Tools Used in Nail Forming and Stamping: A Viability Study, *Matér. Rio J.*, 2021, **26**, p 456. https://doi.org/10.1590/S1517-707620210001.1222
24. O. Gokcekaya, C. Ergun, T. Gulmez, T. Nakano, and S. Yilmaz, Structural Characterization of Ion Nitrided 316L Austenitic Stainless Steel: Influence of Treatment Temperature and Time, *Metals*, 2022, **12**(2), p 306.
25. L. Gil, S. Brühl, L. Jiménez, O. Leon, R. Guevara, and M.H. Staia, Corrosion Performance of the Plasma Nitrided 316L Stainless Steel, *Surf. Coat. Technol.*, 2006, **201**(7), p 4424–4429.
26. E. Roliński, Effect of Plasma Nitriding Temperature on Surface Properties of Austenitic Stainless Steel, *Surf. Eng.*, 1987, **3**(1), p 35–40.
27. A. Nishimoto and K. Nakazawa, Effect of Sample Mount on Active Screen Plasma Duplex Processing, *Mater. Sci. Forum Trans. Tech. Publ. Ltd*, 2014, **782**, p 16–22.
28. M. Ossowski, T. Borowski, M. Tarnowski, and T. Wierzchon, Cathodic Cage Plasma Nitriding of Ti_6Al_4V Alloy, *Mater. Sci.*, 2016, **22**(1), p 25–30.
29. L.C. Silva, M.S. Libório, L.L.F. Lima, R.R.M. Sousa, T.H.C. Costa, M. Naeem, D.A.P. Reis, P.A. Radi, and S.M. Alves, Deposition of MoS_2-TiN Multilayer Films on 1045 Steel to Improve Common Rail Injection System, *J. Mater. Eng. Perform.*, 2020, **29**(10), p 6740–6747.
30. R.F. Lopes, J.A.P. da Costa, W. Silva, B.C. Viana, F.R. Marciano, A.O. Lobo, and R.R.M. Sousa, TiO_2 Anti-Corrosive Thin Films on Duplex Stainless Steel Grown Using Cathodic Cage Plasma Deposition, *Surf. Coat. Technol.*, 2018, **347**, p 136–141.
31. A.G.F. Araújo, M. Naeem, L.N.M. Araújo, T.H.C. Costa, K.H. Khan, J.C. Díaz-Guillén, J. Iqbal, M.S. Liborio, and R.R.M. Sousa, Design, Manufacturing and Plasma Nitriding of AISI-M_2 Steel Forming Tool and Its Performance Analysis, *J. Mater. Res.*, 2020, **9**(6), p 14517–14527.
32. E. Broitman, Indentation Hardness Measurements at Macro- Micro-, and Nanoscale: A Critical Overview, *Tribol Lett*, 2016, **65**(1), p 23.
33. M. Jamil, N. He, X. Huang, W. Zhao, M.K. Gupta, and A.M. Khan, Measurement of Machining Characteristics under Novel Dry Ice Blasting Cooling Assisted Milling of AISI 52100 Tool Steel, *Measurement*, 2022, **191**, p 110821.
34. H.S. Silva, F.R. Marciano, A.S. de Menezes, T.H.C. Costa, L.S. Almeida, L.S. Rossino, I.O. Nascimento, R.R.M. Sousa, and B.C. Viana, Morphological Analysis of the TiN Thin Film Deposited by CCPN Technique, *J. Mater. Res. Technol.*, 2020, **9**(6), p 13945–13955.
35. P.R.Q. de Almeida, P.L.C. Serra, M.R. Danelon, L.S. Rossino, T.H.C. Costa, M.C. Feitor, A.S. de Menezes, R.M. Nascimento, R.M. Sousa, and F.R. Marciano, Plasma Duplex Treatment Influence on the Tribological Properties of the UNS S32760 Stainless Steel, *Surf. Coat. Technol.*, 2021, **426**, p 127774.
36. A.G.F. Araújo, M. Naeem, L.N.M. Araújo, M.S. Libório, M.R. Danelon, R.M. Monção, L.S. Rossino, M.C. Feitor, and R.M. do Nascimento, T.H.C. Costa, and R.R.M. Sousa, Duplex Treatment with Hastelloy Cage on AISI 5160 Steel Cutting Tools, *Mater. Sci. Technol.*, 2022, **38**(8), p 499–506.
37. R.M. Monção, M.R. Danelon, L.S. Almeida, L.S. Rossino, F.R. Marciano, T.H.C. Costa, M.C. Feitor, R.M. Nascimento, and R.R.M. Sousa, Molybdenum Oxide Coatings Deposited on Plasma Nitrided Surfaces, *Mat. Res.*, 2022 https://doi.org/10.1590/1980-5373-MR-2021-0469
38. R.C. Cozza, Estudo da obtenção do Regime Permanente de Desgaste em ensaios de desgaste micro-abrasivo por esfera rotativa conduzidos em corpos-de-prova de WC-Co P_{20} e aço-ferramenta M_2, *Matéria Rio J.*, 2018 https://doi.org/10.1590/S1517-707620170001.0322
39. R.I. Trezona, D.N. Allsopp, and I.M. Hutchings, Transitions between Two-Body and Three-Body Abrasive Wear: Influence of Test Conditions in the Microscale Abrasive Wear Test, *Wear*, 1999, **225–229**, p 205–214.
40. S. Ichimura, S. Takashima, I. Tsuru, D. Ohkubo, H. Matsuo, and M. Goto, Application and Evaluation of Nitriding Treatment Using Active Screen Plasma, *Surf. Coat. Technol.*, 2019, **374**, p 210–221.
41. M.S. Libório, E.O. Almeida, S.M. Alves, T.H.C. Costa, M.C. Feitor, R.M. Nascimento, R.R.M. Sousa, M. Naeem, and M. Jelani, Enhanced Surface Properties of M_2 Steel by Plasma Nitriding Pre-Treatment and Magnetron Sputtered TiN Coating, *Int. J. Surf. Sci. Eng.*, 2020, **14**(4), p 288–306.
42. Y.E. Núñez de la Rosa, O. Palma Calabokis, P.C. Borges, and V. Ballesteros Ballesteros, Effect of Low-Temperature Plasma Nitriding on Corrosion and Surface Properties of Duplex Stainless Steel UNS S32205, *J. Mater. Eng. Perform*, 2020, **29**(4), p 2612–2622.
43. O. Palma Calabokis, Y. Núñez de la Rosa, C.M. Lepienski, R. Perito Cardoso, and P.C. Borges, Crevice and Pitting Corrosion of Low Temperature Plasma Nitrided UNS S32750 Super Duplex Stainless Steel, *Surf. Coat. Technol.*, 2021, **413**, p 127095.
44. J.O. Pereira Neto, R.O. da Silva, E.H. da Silva, J.A. Moreto, R.M. Bandeira, M.D. Manfrinato, and L.S. Rossino, Wear and Corrosion Study of Plasma Nitriding F53 Super Duplex Stainless Steel, *Mat. Res.*, 2016, **19**, p 1241–1252.
45. W.R. de Oliveira, B.C.E.S. Kurelo, D.G. Ditzel, F.C. Serbena, C.E. Foerster, and G.B. de Souza, On the S-Phase Formation and the Balanced Plasma Nitriding of Austenitic-Ferritic Super Duplex Stainless Steel, *Appl. Surf. Sci.*, 2018, **434**, p 1161–1174.
46. J. Olsson and M. Snis, Duplex — A New Generation of Stainless Steels for Desalination Plants, *Desalination*, 2007, **205**(1), p 104–113.
47. R.A. Andrade and R. Magnabosco, Computational Simulation of Duplex Stainless Steel Continuous Cooling Transformation Curves Using DICTRA®, *Mat. Res.*, 2022 https://doi.org/10.1590/1980-5373-MR-2021-0593
48. D.K. Prajapati and M. Tiwari, The Correlation between Friction Coefficient and Areal Topography Parameters for AISI 304 Steel Sliding against AISI 52100 Steel, *Friction*, 2021, **9**(1), p 41–60.
49. M.S. Libório, G.B. Praxedes, L.L.F. Lima, I.G. Nascimento, R.R.M. Sousa, M. Naeem, T.H. Costa, S.M. Alves, and J. Iqbal, Surface Modification of M_2 Steel by Combination of Cathodic Cage Plasma Deposition and Magnetron Sputtered MoS_2-TiN Multilayer Coatings, *Surf. Coat. Technol.*, 2020, **384**, p 125327.